



**SPE 124332**

## **Hierarchical Long-Term and Short-Term Production Optimization**

G.M. van Essen, SPE; P.M.J. Van den Hof, Delft University of Technology (TU Delft); J.D. Jansen, SPE, TU Delft and Shell International E&P

Copyright 2009, Society of Petroleum Engineers

This paper was prepared for presentation at the 2009 SPE Annual Technical Conference and Exhibition held in New Orleans, Louisiana, USA, 4–7 October 2009.

This paper was selected for presentation by an SPE program committee following review of information contained in an abstract submitted by the author(s). Contents of the paper have not been reviewed by the Society of Petroleum Engineers and are subject to correction by the author(s). The material does not necessarily reflect any position of the Society of Petroleum Engineers, its officers, or members. Electronic reproduction, distribution, or storage of any part of this paper without the written consent of the Society of Petroleum Engineers is prohibited. Permission to reproduce in print is restricted to an abstract of not more than 300 words; illustrations may not be copied. The abstract must contain conspicuous acknowledgment of SPE copyright.

---

### **Abstract**

Model-based dynamic optimization of oil production has a significant potential to improve economic life-cycle performance, as has been shown in various studies. However, within these studies short-term operational objectives are generally neglected. As a result, the optimized injection and production rates often result in a considerable decrease in short-term production performance. In reality however, it is often these short-term objectives that dictate the course of the operational strategy. Incorporating short-term goals into the life-cycle optimization problem is therefore an essential step in model-based life-cycle optimization. We propose a hierarchical optimization structure with multiple objectives. Within this framework, the life-cycle performance in terms of net present value (NPV) serves as primary objective and short-term operational performance is the secondary objective, such that optimality of the primary objective constrains the secondary optimization problem. This requires that optimality of the primary objective does not fix all degrees of freedom (DOF) of the decision variable space. Fortunately, the life-cycle optimization problem is generally ill-posed and contains many more decision variables than necessary. We present a method that identifies the redundant DOF in the life-cycle optimization problem, which can subsequently be used in the secondary optimization problem. In our study we used a 3-dimensional reservoir in a fluvial depositional environment with a production life of 7 years. The primary objective is undiscounted NPV, while the secondary objective is aimed at maximizing short-term production. The optimal life-cycle waterflooding strategy that includes short-term performance is compared to the optimal strategy that disregards short-term performance. The experiment shows a very large increase in short-term production, boosting first year production by a factor 2, without significantly compromising optimality of the primary objective, showing a slight drop in NPV of only  $-0.3\%$ . Our method to determine the redundant DOF in the primary objective function relies on the computation of the Hessian matrix of the objective function with respect to the control variables. Although theoretically rigorous, this method is computationally infeasible for realistically sized problems. We therefore also developed a second, more pragmatic, method relying on an alternating sequence of optimizing the primary and secondary objective functions. Subsequently we demonstrated that both methods lead to nearly identical results, which offers scope for application of hierarchical long-term and short-term production optimization to realistically sized flooding optimization problems.

### **Introduction**

Over the recent years, improvements in dynamic reservoir modeling and measurement and control capabilities have led to an increased interest in model-based operation of oil fields. Several studies have shown that there may be a significant scope for improving reservoir management by using reservoir models to optimize economic life-cycle performance; see e.g. Asheim (1988), Sudaryanto and Yortsos (2000), Brouwer and Jansen (2004) and Sarma et al. (2005). Especially combined with methods to reduce uncertainty – referred to as closed-loop reservoir management, see e.g. Naevdal et al. (2006), Sarma et al. (2008), Chen et al. (2008), Jansen et al. (2009) and Wang et al. (2009) – these (proactive) life-cycle optimization techniques seem to be a promising alternative to more reactive approaches, which are current practice.

However, in these studies on improved life-cycle performance the importance of meeting short-term targets, e.g. maximizing revenues over a short time interval, are generally neglected. As a result, many of the improvements in life-cycle performance are obtained at the expense of short-term objectives. In reality however, it is often these short-term objectives

that dictate the course of the operational strategy, especially in view of geological and economic uncertainties. Incorporating short-term goals into the life-cycle optimization problem is therefore an essential step in the route towards implementation of the closed-loop reservoir management concept. To this end, Saputelli et al. (2005, 2006) proposed a multi-level hierarchical control structure, where the separation of the levels was based on different time-scales and objectives.

Jansen et al. (2009) observed that significantly different optimized waterflooding strategies result in nearly equal values in NPV. They concluded that the life-cycle optimization problem is ill-posed and contains many more control variables than necessary. As a result, there exist multiple solutions to the optimization problem, and different initial guesses of an input  $\mathbf{u}$  may lead to different solution points in an optimal subset  $\mathcal{S}$  of the decision variable space  $\mathcal{U}$ .

The goal to this paper is to present a hierarchical optimization framework that is able to address both short-term as long-term objectives in a consistent manner. Although this framework is generic in nature, the presented approach is aimed at maximizing an economic life-cycle objective, in terms of NPV, without disregarding short-term performance. The existence and nature of multiple solutions in the life-cycle optimization problem is investigated as they provide the possibility to improve short-term operational goals, while aiming for economic life-cycle optimality.

### Life-Cycle Optimization Problem

The life-cycle (i.e. long-term) optimization problem does not impose any particular choice of depletion or modeling technique. It only requires the existence of at least one decision variable and the model being capable of providing relatively reliable long-term predictions. However, in many case studies waterflooding is selected as depletion method for a number of reasons:

- It is a common recovery mechanism.
- A waterflooding strategy involves many decision variables.
- The flooding process can be modeled reasonably accurate over long distances and periods of time.
- There is generally a significant scope for improvement.

For these reasons, waterflooding is also adopted as production process within this work. However, the mathematical formulation is kept generic as far as possible. Due to the transient nature of the saturation distribution in an oil-producing reservoir, dynamic optimization must be performed over the entire life of the reservoir to improve economic life-cycle performance. This optimization problem can be expressed by the following mathematical formulation:

$$\max_{\mathbf{u}_{1:K}} J(\mathbf{u}_k), \quad (1)$$

$$s.t. \quad \mathbf{g}_{k+1}(\mathbf{u}_k, \mathbf{x}_k, \mathbf{x}_{k+1}) = \mathbf{0}, \quad k = 0, \dots, K-1, \quad \mathbf{x}_0 = \bar{\mathbf{x}}_0, \quad (2)$$

$$\mathbf{c}_{k+1}(\mathbf{u}_{k+1}, \mathbf{x}_{k+1}) \leq \mathbf{0}, \quad (3)$$

where  $\mathbf{u}$  is the control vector (input vector),  $\mathbf{x}$  is the state vector (grid block pressures and saturations),  $\mathbf{g}$  is a vector-valued function that represents the system equations,  $\mathbf{x}_0$  is a vector of the initial conditions of the reservoir, the subscript  $k$  indicates discrete time, and  $K$  is the total number of time step. A colon in a subscript indicates a range, e.g.  $\mathbf{u}_{1:K} = \{\mathbf{u}_1, \mathbf{u}_2, \dots, \mathbf{u}_K\}$ . The vector of inequality constraints  $\mathbf{c}$  relates to the capacity limitations of the wells. The objective function  $J$  is of an economic type, generally Net Present Value:

$$J = \sum_{k=1}^K \left[ \frac{\sum_{i=1}^{N_{inj}} r_{wi} \cdot (u_{wi,i})_k - \sum_{j=1}^{N_{prod}} [r_{wp} \cdot (y_{wp,j})_k + r_o \cdot (y_{o,j})_k]}{(1+b)^{\frac{t_k}{\tau_t}}} \cdot \Delta t_k \right], \quad (4)$$

where  $r_o$  is the oil revenue (with units  $\$/\text{m}^3$ ),  $r_{wp}$  the water production costs ( $\$/\text{m}^3$ ) and  $r_{wi}$  the water injection costs ( $\$/\text{m}^3$ ), which are all assumed constant.  $\Delta t_k$  is the time interval of time step  $k$  in days. The term  $b$  represents the discount rate for a certain reference time  $\tau_t$ . The terms  $N_{inj}$  and  $N_{prod}$  relate to the number of injection wells and production wells respectively. In Equation 4, the output variables  $y_{wp,j}$  and  $y_{o,j}$  relate to the water production rate and oil production rate of well  $j$ , which form part of the output vector

$$\mathbf{y}_{k+1} = \mathbf{h}(\mathbf{u}_{k+1}, \mathbf{x}_{k+1}), \quad (5)$$

with  $\mathbf{h}$  a vector-valued output function that relates  $\mathbf{y}$  to the control vector (input vector)  $\mathbf{u}$  and the state  $\mathbf{x}$ . The term  $u_{wi,i}$  represents those elements of  $\mathbf{u}$  that involve the water injection flow rates of well  $i$ . An economic objective functions like (4) does not necessarily provide a unique solution to the optimization problem. Although it relates to realistic business conditions, it may well cause ill-posedness of the problem.

Several methods exist to attack the dynamic optimization problem of batch-like processes; see e.g. Srinivasan et al. (2003). However, the size of the waterflooding optimization problem (1) – (3) limits the possibilities. Simultaneous methods or dynamic programming are impractical due to the usually very large number of states of reservoir models. The resulting long simulation times and large number of input variables also rule out search methods that require many function evaluations, e.g. genetic algorithms. A viable optimization technique is a gradient-based method using a set of adjoint equations to determine the gradients; see e.g. Brouwer and Jansen (2004), Sarma et al. (2005) and Kraaijevanger et al. (2007). This approach to life-cycle waterflooding optimization is encountered most often in literature and is also the method implemented in the proprietary reservoir simulator used in this study.

## Hierarchical Optimization

### Multiple Objectives

In the life-cycle waterflooding problem as expressed by (1) – (3), the desire to aim for maximal short-term (daily) production is discarded. A balanced objective provides a possibility to address both objectives in a single function, see Marler and Arora (2004):

$$J_{bal} = \omega_1 \cdot J_1 + \omega_2 \cdot J_2. \quad (6)$$

Here  $J_{bal}$  is the balanced objective function constructed from the weighted long-term and short-term objective functions  $J_1$  and  $J_2$ . The terms  $\omega_1$  and  $\omega_2$  are weighting factors of respectively the short- and long-term objective. When using the balanced objective function, finding suitable weighting factors between the objectives may prove to be difficult. This is especially the case if the values of the multiple objective functions have different physical interpretations.

Alternatively, we propose a hierarchical optimization structure – sometimes referred to as the *lexicographic* method – that requires a prioritization of the multiple objectives, as described in Haimes and Li (1988). In this structure, optimization of a secondary objective function  $J_2$  is constrained by the requirement that the primary objective function  $J_1$  must remain close to its optimal value  $J_1^*$ . This structure can be expressed mathematically as follows:

$$\max_{\mathbf{u}_k} J_2(\mathbf{u}_k), \quad (7)$$

$$s.t. \quad \mathbf{g}_{k+1}(\mathbf{u}_k, \mathbf{x}_k, \mathbf{x}_{k+1}) = \mathbf{0}, \quad k = 0, \dots, K-1, \quad \mathbf{x}_0 = \bar{\mathbf{x}}_0, \quad (8)$$

$$\mathbf{c}_{k+1}(\mathbf{u}_{k+1}, \mathbf{x}_{k+1}) \leq \mathbf{0}, \quad (9)$$

$$J_1^* - J_1(\mathbf{u}_{k+1}) \leq \varepsilon, \quad (10)$$

where  $\varepsilon$  is an arbitrary small value compared to  $J_1^*$ . Solving (7) – (10) requires the knowledge of  $J_1^*$ , which is obtained through solving optimization problem (1) – (3). In the hierarchical optimization structure (7) – (10), the optimum value of the life-cycle objective function  $J_1$  constrains optimization of the short-term objective. It should be noted that this ordering of long- and short term is by no means unique. Alternatively, one may want to optimize life-cycle performance under the condition that certain short-term production targets are met. In that case, the short-term goals act as constraints on the life-cycle optimization problem.

### Redundant Degrees of Freedom

Jansen et al. (2009) described that there exist different solutions to the optimal control problem of maximizing an economic objective function over the life of the reservoir. The existence of multiple solutions was attributed to the ill-posedness of the optimal control problem. The ill-posedness also suggests that even when optimality of an economic life-cycle objective is reached, not all degrees of freedom (DOF) of the decision variable space  $\mathcal{U}$  are fixed and the solution points in the optimal subset  $\mathcal{S}$  are connected. This means that there may exist redundant DOF in the optimization problem. Huesman et al. (2006) found similar results for economic dynamic optimization of plant-wide operation. A consequence of these redundant DOF is that even if  $\varepsilon$  in (10) is chosen equal to 0, DOF are left to improve the secondary objective function  $J_2$ . A straightforward way of investigating this is to imbed (10) as an equality constraint in the adjoint formulation by means of an additional Lagrange multiplier. Unfortunately, the adjoint functionality in the simulator used in our study was not yet capable of dealing with

(additional) state constraints. Alternatively, unconstrained gradient information can be used to investigate the redundant DOF, as described in the next section.

### Quadratic Approximation of the Objective Function

In the following we will use the short-cut notation  $\mathbf{u}$  to indicate the input sequence  $\mathbf{u}_{1:K} = \{\mathbf{u}_1, \mathbf{u}_2, \dots, \mathbf{u}_K\}$ . A solution  $\mathbf{u}$  for which no constraints are active is an optimal solution  $\mathbf{u}^*$  if and only if the gradients of  $J$  with respect to  $\mathbf{u}$  are zero, i.e.  $[\partial J / \partial \mathbf{u}]^T = \mathbf{0}$ . As a result, at  $\mathbf{u}^*$  the gradients do not provide any information on possible redundant degrees of freedom under the optimality condition on  $J$ . Second-order derivatives of  $J$  with respect to  $\mathbf{u}$  are collected in the Hessian matrix  $\mathbf{H} = \partial^2 J / \partial \mathbf{u}^2$ . If  $\mathbf{H}$  is negative-definite, the considered solution  $\mathbf{u}$  is an optimal solution, but no DOF are left when the optimality condition on  $J$  holds. If  $\mathbf{H}$  is negative-semidefinite it means that the Hessian does not have full rank. An orthonormal basis  $\mathbf{B}$  for the undetermined directions of  $\mathbf{H}$  can then be obtained through a singular value decomposition:

$$\mathbf{H} = \mathbf{U}\mathbf{\Sigma}\mathbf{V}^T. \quad (11)$$

The orthonormal basis  $\mathbf{B}$  consists of those columns of  $\mathbf{V}$  that relate to singular values of zero, i.e.:

$$\mathbf{B} \triangleq \{\mathbf{v}_i \mid \sigma_i = 0, \quad i = 1, \dots, N_{\mathbf{u}}\}, \quad (12)$$

where  $\mathbf{v}_i$  is the  $i^{\text{th}}$  column of  $\mathbf{V}$ ,  $\sigma_i$  is the  $i^{\text{th}}$  singular value and  $N_{\mathbf{u}}$  is the number of DOF in the input. Note that due to the symmetrical nature of the Hessian matrix  $\mathbf{H}$ , the singular value decomposition may be replaced by a, computationally more efficient, eigenvalue decomposition, in which case the eigenvectors relating to eigenvalues equal to zero span the orthonormal basis  $\mathbf{B}$ .

Not all orthogonal directions spanned by the columns of  $\mathbf{B}$  will be redundant DOF. These directions are redundant DOF, if they are linear and if all higher-order derivatives are zero as well, which at this point in time is impossible to prove for reservoir models.  $\mathbf{B}$  is however a basis for redundant DOF for a quadratic approximation  $\hat{J}$  of objective function  $J$ . As  $\hat{J}$  can be considered to be an acceptable approximation for small deviations from  $\mathbf{u}^*$ ,  $\mathbf{B}$  can be regarded as an acceptable basis for the redundant DOF for small deviations from  $\mathbf{u}^*$ .

### Approximate Hessian Matrix

Unfortunately, no reservoir simulation package is currently capable of calculating second-order derivatives. However, using the gradient information, second-order derivatives can be approximated. In our study we used a forward-difference scheme:

$$\frac{\partial^2 J}{\partial u_i \partial u_j} \approx \frac{\nabla J_i(\mathbf{u} + h_j \mathbf{e}_j) - \nabla J_i(\mathbf{u})}{2h_j} + \frac{\nabla J_j(\mathbf{u} + h_i \mathbf{e}_i) - \nabla J_j(\mathbf{u})}{2h_i}, \quad (13)$$

where  $\nabla J_i$  is the  $i^{\text{th}}$  element of the gradient  $\nabla J = [\partial J / \partial \mathbf{u}]^T$ ,  $\mathbf{e}_i$  is a canonical unit vector, i.e. a vector with a 1 at element  $i$  and 0 elsewhere and  $h_i$  is the perturbation step size that relates to parameter  $u_i$  of  $\mathbf{u}$ . In total  $N_{\mathbf{u}}+1$  simulations (function evaluations) are required to obtain the approximate Hessian matrix  $\hat{\mathbf{H}}$  at a particular optimal solution  $\mathbf{u}^*$ .

Alternatively, a reduced Hessian method could be used that approximates only that portion of the Hessian relevant for the subspace in which the Hessian is negative (or positive) definite, see Byrd and Nocedal (1990). If the Hessian is negative (or positive) semidefinite, the tangent space of this subspace will be equal to the null-space of the complete Hessian matrix. This could lead to a significant reduction in computational burden, especially when the dimensions of the null-space are large.

### Hierarchical Optimization Method

Adopting the approximation of  $\mathbf{H}$  as described in the previous subsection, the following iterative procedure is proposed to attack the hierarchical optimization problem (7) – (10) with  $\varepsilon = 0$ :

- 1) Find a (single) optimal strategy  $\mathbf{u}^*$  that maximizes the primary objective function  $J_1$  and use  $\mathbf{u} = \mathbf{u}^*$  as starting point in the secondary optimization problem.
- 2) Approximate the Hessian matrix  $\mathbf{H}$  of  $J_1$  with respect to the input variables at (initial input)  $\mathbf{u}$  and determine an orthonormal basis  $\mathbf{B}$  for the null-space of  $\hat{\mathbf{H}}$ .
- 3) Find the improving gradient direction  $\partial J_2 / \partial \mathbf{u}$  for the secondary objective function  $J_2$ .
- 4) Project  $\partial J_2 / \partial \mathbf{u}$  onto the orthonormal basis  $\mathbf{B}$  to obtain projected direction  $\mathbf{d}$ , such that  $\mathbf{d}$  is an improving direction for  $J_2$ , but does not affect  $J_1$ . The projection is performed using projection matrix  $\mathbf{P}$  according to

$$\mathbf{d} = \mathbf{P} \cdot \left( \frac{\partial J_2}{\partial \mathbf{u}} \right)^T, \quad (14)$$

$$\mathbf{P} = \mathbf{B}\mathbf{B}^T. \quad (15)$$

- 5) Update  $\mathbf{u}$  using projected direction  $\mathbf{d}$  in a steepest ascent method

$$\mathbf{u}_{n+1} = \mathbf{u}_n + \tau \cdot \mathbf{d}, \quad (16)$$

where  $\tau$  is an appropriately small step size such that the quadratic approximation of  $J_1$  is justified and  $n$  is the iteration index.

- 6) Perform steps 2 through 6 until convergence of  $J_2$ .

In the next section a numerical example will be presented where the iterative hierarchical optimization structure is tested on a 3D heterogeneous reservoir model.

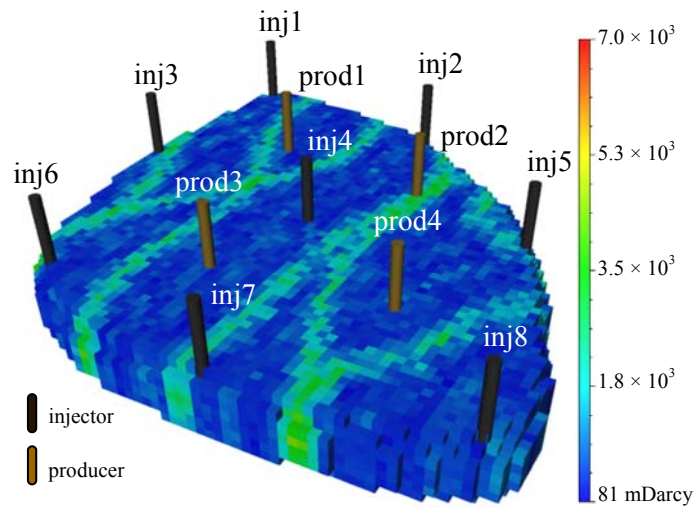


Fig. 1: 3-dimensional oil reservoir model (van Essen et al. 2006).

### Example

We applied the hierarchical optimization procedure to a 3-dimensional oil reservoir model, introduced in Van Essen et al. (2006). The life-cycle of the reservoir covers a period of 3,600 days. The reservoir model consists of 18,553 grid blocks, as depicted in **Fig. 1**, and has dimensions of 480×480×28 meter. Its geological structure involves a network of fossilized meandering channels. The average reservoir pressure is 400 bar. All remaining geological and fluid properties used in this example are presented in **Table 1**.

Table 1 – Geological and fluid properties example		
<u>property</u>	<u>value</u>	<u>units</u>
$\phi$	0.20	-
$\rho_o$ (@1 bar)	900	kg/m <sup>3</sup>
$\rho_w$ (@1 bar)	1000	kg/m <sup>3</sup>
$c_o$	$1 \times 10^{-5}$	1/bar
$c_w$	$1 \times 10^{-5}$	1/bar
$\mu_o$	$5 \times 10^{-3}$	Pa s
$\mu_w$	$1 \times 10^{-3}$	Pa s
$p_{cow}$	0	bar

The reservoir model contains 8 injection wells and 4 production wells. The production wells are modeled using a standard Peaceman well model, which relates the source (output) term  $\mathbf{y}$ , to the pressure difference between the well and grid block pressure:

$$y_k^j = w_j \cdot (p_{wf,k}^j - p_k^j), \quad (17)$$

where  $p_{wf}$  is the flowing wellbore pressure (bottom hole pressure),  $j$  the index of the grid block containing the well and  $p_k^j$  the grid block pressure in which the well is located. The well index  $w_j$  is a constant, which contains the well's geometric factors and the rock and fluid properties of the reservoir directly around the well. The wells operate at a constant bottom hole pressure  $p_{wf}$  of 395 bar. The flow rates of the injection wells can be manipulated directly, i.e. the control input  $\mathbf{u}$  involves injection flow rate trajectories for each of the 8 injection wells. The minimum rate for each injection well is  $0.0 \text{ m}^3/\text{day}$ , the maximum rate is set at a rate of  $79.5 \text{ m}^3/\text{day}$ . The control input  $\mathbf{u}$  is re-parameterized in time using a zero-order-hold scheme with input parameter vector  $\boldsymbol{\theta}$ . For each of the 8 injection wells, the control input  $\mathbf{u}$  is re-parameterized into 4 time periods  $t_{\theta}$  of 900 days over which the injection rate is held constant at value  $\theta_i$ . Thus, the input parameter vector  $\boldsymbol{\theta}$  consists of  $8 \times 4 = 32$  elements.

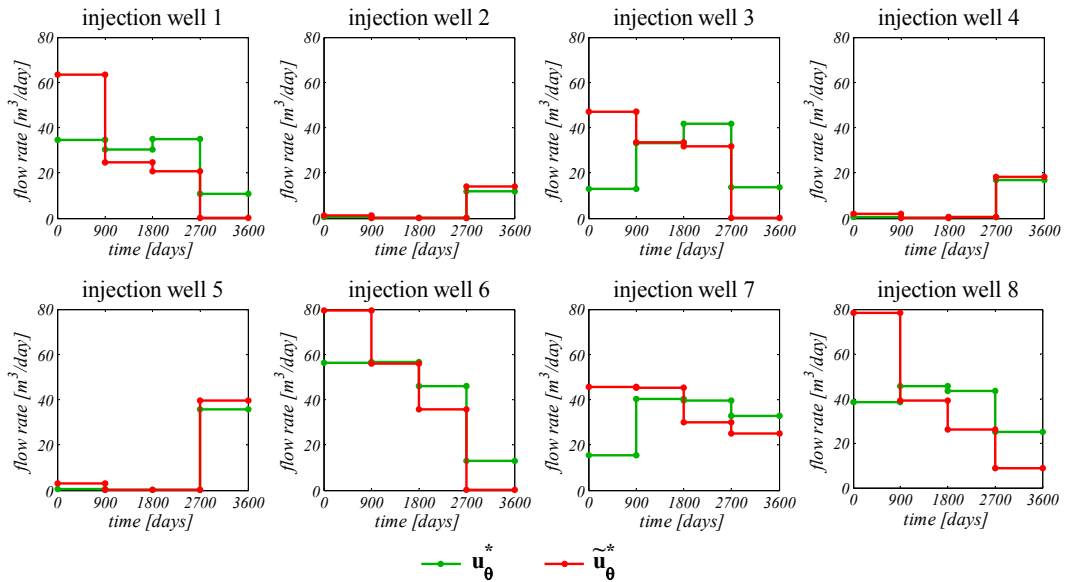


Fig. 2: Input trajectories for each of the 8 injection wells for the initial optimal solution  $\mathbf{u}_0^*$  to  $J_1$  (green) and the optimal solution  $\tilde{\mathbf{u}}_0^*$  after the constrained optimization of  $J_2$  (red)

### Life-Cycle Optimization

The objective function for the life-cycle optimization was defined in terms of NPV, as defined in Equation (4), with  $r_o = 126 \text{ \$/m}^3$ ,  $r_{wp} = 19 \text{ \$/m}^3$  and  $r_{wi} = 6 \text{ \$/m}^3$ . The discount rate  $b$  was set to 0. Thus, the life-cycle objective relates to undiscounted cash flow. The optimal input - denoted by  $\mathbf{u}_0^*$  - obtained after approximately 50 iterations using a steepest ascent scheme, is shown in Fig. 2. Note that none of the input constraints (9) is active for  $\mathbf{u}_0^*$ . The value of the objective function corresponding to input  $\mathbf{u}_0^*$  is  $47.6 \times 10^6 \text{ \$}$ .

### Hierarchical Optimization

We defined the secondary objective function  $J_2$  such as to emphasize the importance of short-term production. To that end,  $J_2$  was chosen identical to the primary objective function but with the addition of a very high annual discount rate  $b$  of 0.25. As a result, short-term production is weighed more heavily than future production. Note that due to the extremely high discount rate, the actual value of  $J_2$  no longer has a realistic meaning in an economic sense.

Next, we applied the hierarchical approach as presented in the previous section. The total number of simulation runs needed to approximate the Hessian ( $\hat{\mathbf{H}}$ ) was 33, but the overall simulation time was kept within acceptable limits by parallel processing the simulations. Because this example involves a numerical model and an approximation of the second-order derivatives, we relaxed the selection criterion for  $\mathbf{B}$ . Those columns  $\mathbf{v}_i$  of  $\mathbf{V}$  were selected that correspond to singular values

for which  $\sigma_i/\sigma_1 < 0.02$  instead of  $\sigma_i = 0$ . The projected gradients  $\mathbf{d}$  were again used in a steepest-ascent scheme. In order to ensure that  $\mathbf{u}_{0,m+1}$  remains close to  $\mathbf{u}_{0,m}$ ,  $\mathbf{d}$  was normalized and a constant step size  $\tau$  of 1 was used in the steepest ascent scheme.

Due to computing time restrictions, the hierarchical optimization of  $J_2$  was terminated after 210 iterations with final control input  $\tilde{\mathbf{u}}_0^*$ . To evaluate the results of the hierarchical optimization, the optimization of  $J_2$  was also performed without projection on  $\mathbf{B}$ . As a result, the obtained control input - denoted by  $\tilde{\mathbf{u}}_0$  - in that case does not ensure optimality of  $J_1$ . **Fig. 3** displays the values of  $J_1$  and  $J_2$  plotted against the iteration number for the hierarchical optimization problem. It shows a considerable increase of  $J_2$  of 28.2% and a slight drop of  $J_1$  of -0.3%. In Fig. 2 the input strategy after the final iteration step is presented. It can be observed that the injection strategy shows a substantial increase in injection rates at the beginning of the production life and a decrease at the end.

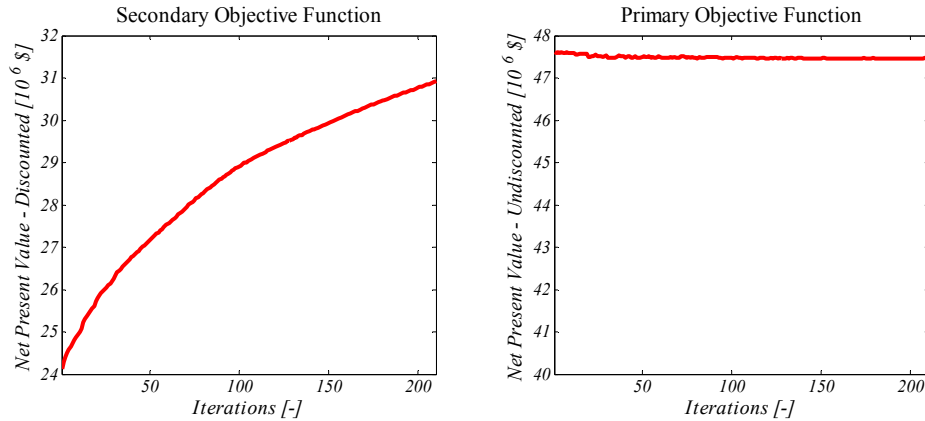


**Fig. 3:** Values of the secondary objective function  $J_2$  and the primary objective function  $J_1$  plotted against the iteration number for the constrained secondary optimization problem.

As a comparison, we repeated the optimization of  $J_2$  starting from  $\mathbf{u}_0^*$  with the difference that it was no longer constrained by requirement that  $J_1$  remains close to  $J_1^*$ , i.e. Equation (10) was omitted. The optimization procedure was terminated after 107 iterations when the improvement of  $J_2$  was equal to 28.2%, i.e. the final value of  $J_2$  in the constrained optimization case. The values of  $J_1$  and  $J_2$  plotted against the iteration number for the unconstrained optimization of  $J_2$  are shown in **Fig. 4**. Again an increase in  $J_2$  of 28.2% is realized, but now at a cost of a decrease in  $J_1$  of -5.0%. Finally, **Fig. 5** shows the value of the primary objective function  $J_1$  over time until the end of the producing reservoir life for  $\mathbf{u}_0^*$ ,  $\tilde{\mathbf{u}}_0^*$  and  $\tilde{\mathbf{u}}_0$ . Input  $\tilde{\mathbf{u}}_0^*$  shows a steeper ascent of  $J_1$  than  $\mathbf{u}_0^*$ , while their final values are nearly equal. Input  $\tilde{\mathbf{u}}_0$  shows initially the same steep ascent as, but  $J_1$  drops towards the end of the life of the reservoir.

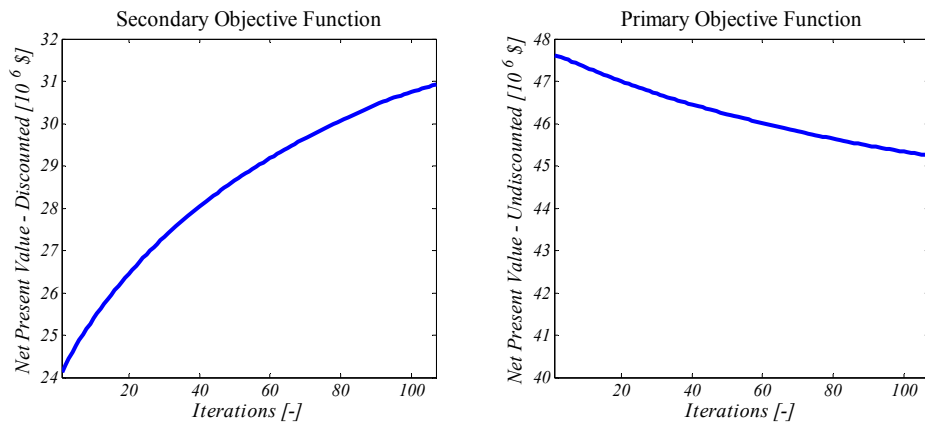


**Fig. 4:** Values of the secondary objective function  $J_2$  and the primary objective function  $J_1$  plotted against the iteration number for the secondary optimization problem, no longer constrained by the orthonormal basis  $\mathbf{B}$ .

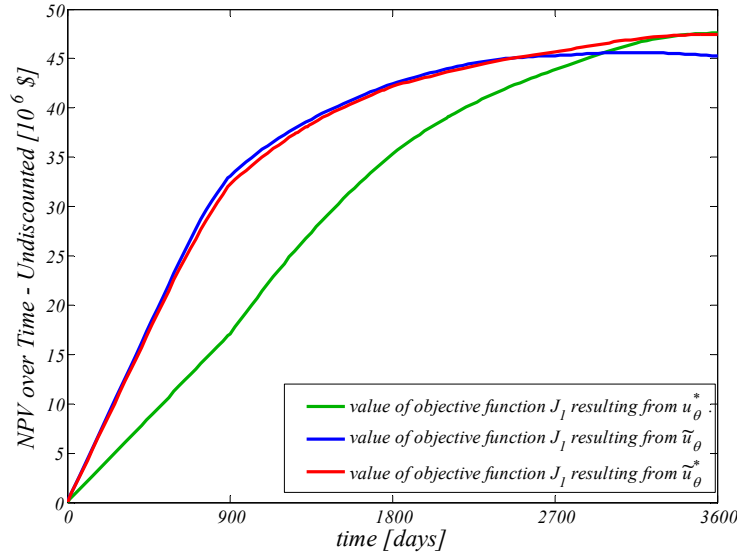


Fig. 5: Value of the primary objective function  $J_1$  over time for initial optimal input  $\mathbf{u}_0^*$  to  $J_1$  (green), the optimal input  $\tilde{\mathbf{u}}_0^*$  after the constrained optimization of  $J_2$  (red) and input  $\tilde{\mathbf{u}}_0$  after the unconstrained optimization of  $J_2$  (blue).

### Alternative Methods

The presented hierarchical optimization approach is computationally very demanding and becomes infeasible for more realistic reservoir models with an increased number of input parameters, even when reduced Hessian techniques are used. It should be noted, however, that execution of the hierarchical optimization procedure does not require knowledge of all redundant DOF explicitly. In theory, the inequality constraint (10) could be incorporated in the adjoint formulation through the use of an additional Lagrange multiplier, by which the calculation of second-order derivatives is avoided altogether. However, this would require modifications to the reservoir simulator, and we therefore did not pursue this route. An alternative method to solve the hierarchical optimization problem without explicitly calculating the redundant DOF is through the use of a balanced objective function as described by Equation (6), with the variation of using weighting functions  $\Omega_1$  and  $\Omega_2$  instead of weighting factors  $\omega_1$  and  $\omega_2$ :

$$J_{bal} = \Omega_1 \cdot J_1 + \Omega_2 \cdot J_2. \quad (18)$$

where  $\Omega_1$  and  $\Omega_2$  are ‘switching’ functions of  $J_1$  and  $J_1^*$  that take on values of 1 and 0 or vice versa:

$$\Omega_1(J_1) = \begin{cases} 1 & \text{if } J_1 < \varepsilon \\ 0 & \text{if } J_1 \geq \varepsilon \end{cases}, \quad \Omega_2(J_1) = \begin{cases} 0 & \text{if } J_1 < \varepsilon \\ 1 & \text{if } J_1 \geq \varepsilon \end{cases}. \quad (19)$$

Here,  $\varepsilon$  is the threshold value as defined in inequality constraint (10). The gradient of  $J_{bal}$  with respect to the input parameters  $\mathbf{u}$  for iteration  $n+1$  is then simply:

$$\left. \frac{\partial J_{bal}}{\partial \mathbf{u}} \right|_{n+1} = \Omega_1(J_{1,n}) \cdot \left. \frac{\partial J_1}{\partial \mathbf{u}} \right|_{n+1} + \Omega_2(J_{1,n}) \cdot \left. \frac{\partial J_2}{\partial \mathbf{u}} \right|_{n+1}. \quad (20)$$

Execution of the optimization problem using balanced objective function (18), sequentially gives improving directions for either  $J_1$  or  $J_2$ . With each iteration, the value of  $J_2$  either increases while the value of  $J_1$  decreases or the other way around, as the solution moves to and from the feasible region with respect to inequality constraint (10). When no redundant DOF are available, the control input would hop between two fixed solutions, of which only one would be feasible. However, in the

case that redundant DOF do exist, improvement of  $J_2$  is possible without compromising (10) and convergence of the hierarchical optimization will occur in a ‘zig-zag’ fashion, as schematically represented in Fig. .

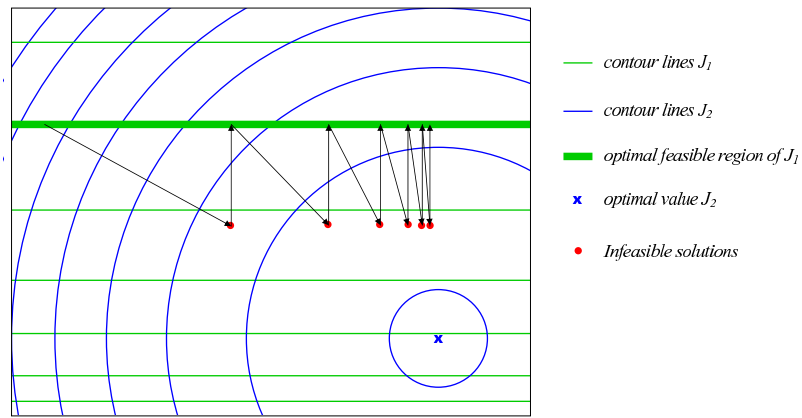


**Fig. 6: Schematic representation of the iterative process of solving a hierarchical optimization problem using an objective function as described by (18) – (19). The process converges towards a final solution in a ‘zig-zag’-fashion , moving into and out of the feasible region bounded by the optimal solutions of the primary objective function  $J_1$ .**

This ‘switching’ method has the advantage that numerous evaluations of the system and adjoint equations are avoided: only 2 (parallelly executed) runs of the system and adjoint equations are necessary per iterations, regardless of the number of input parameters. Secondly, the method is straightforward to implement. Finally, it provides the possibility to explicitly set a bound on the deviation of  $J_1$  from  $J_1^*$  by choosing an appropriate value for  $\epsilon$ . A disadvantage of the method is the slow convergence due to the infeasible solution steps. Also, some tuning of  $\tau$  will be required to account for the fact that the Euclidean length of vectors  $\partial J_1/\partial \mathbf{u}$  and  $\partial J_2/\partial \mathbf{u}$  is different.

**Example**

The switching method was again applied to the 3-dimensional oil reservoir model. Although the number of input parameters does not pose a problem to the switching method, again the control input was parameterized using 32 parameters to allow for a fair comparison with previous results. For the choice of threshold value  $\epsilon$ , the maximum deviation of  $J_1$  from  $J_1^*$  from the null-space method was used (-0.3%), i.e.  $\epsilon = 0.997 \times J_1^*$ . Just as in the null-space example, optimization of  $J_2$  using objective function (18) was started from  $\mathbf{u}_0^*$ . The optimization procedure was again terminated when a feasible solution was found that gave an improvement of  $J_2$  of 28.2%. The results of the hierarchical optimization problem using the switching method are shown in Fig. 7.

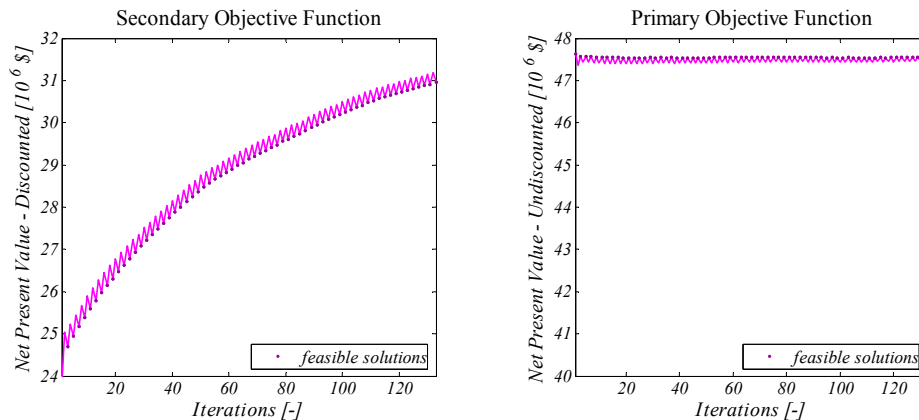


**Fig. 7: Values of the secondary objective function  $J_2$  and the primary objective function  $J_1$  plotted against the iteration number for the secondary optimization problem, using the switching methods. The ‘feasible solutions’ marks relate to those solutions that are feasible with respect to inequality constraint (10).**

Fig. 7 shows that the switching method is able to give similar results for the hierarchical optimization problem as the null-space method. Note however that not only much fewer evaluations of the system and adjoint equations per iteration are required (2 versus 33), but that also the number of required iterations is smaller (140 versus 210)..

## Discussion and Conclusions

### Discussion

In the hierarchical approach presented in this paper, long-term (life-cycle) recovery optimization was selected as primary objective, while short-term production optimization served as secondary objective. However, the concept of using the redundant DOF of the primary objective to improve a secondary objective is not limited to this specific choice. Alternatively, the secondary objective function may be used to e.g. search for a more smooth production profile, a bang-bang production profile; see Zandvliet et al. (2006), or a persistently exciting production profile; see Zandvliet et al. (2008). Also, a different primary objective function may be chosen, e.g. ultimate recovery or short-term production, provided that it offers enough redundant DOF to improve a secondary objective function.

### Conclusions

We addressed the issue of multiple (long-term and short-term) objectives in oil production optimization and investigated a hierarchical approach by means of a numerical experiment. Based on this experiment we conclude that:

- There exist redundant degrees of freedom (DOF) in the input strategy  $\mathbf{u}$  with respect to the optimality of the long-term objective. This implies the existence of an optimal subset  $\mathcal{S}$  of connected optimal solutions within the solution space  $\mathcal{U}$ .
- The redundant DOF create enough freedom to significantly improve a secondary, short-term, objective function. Moreover, the difference between the initial and final input strategy to the secondary optimization problem is substantial. This suggests that  $\mathcal{S}$  occupies a considerable space within decision variable space  $\mathcal{U}$ .
- The presented hierarchical optimization procedure provides a method to incorporate short-term performance objectives into the problem setting of maximizing life-cycle performance of oil recovery. Using the hierarchical structure, optimization of the secondary objective can be obtained without significantly compromising the primary objective.
- A theoretically rigorous method to select the redundant DOF in the primary objective function requires computation of the Hessian of the objective function with respect to the control variables. This makes the theoretically rigorous method computationally too demanding for application to realistically sized problems.
- Nearly identical results can be obtained with the aid of a somewhat more pragmatic, but computationally much more efficient ‘switching method’ that, starting from an optimal long-term strategy, alternately optimizes the primary and secondary objective functions.

### Acknowledgements

This research was carried out within the context of the Integrated Systems Approach to Petroleum Production (ISAPP) knowledge centre. ISAPP is a joint project between Delft University of Technology (TUD), Shell International Exploration and Production (SIEP), and the Dutch Organization for Applied Scientific Research (TNO).

## Nomenclature

$\mathbf{B}$  = basis for redundant DOF  
 $b$  = discount rate  
 $c$  = compression  
 $\mathbf{d}$  = projected search direction on  $\mathbf{B}$   
 $n$  = iteration index  
 $\mathbf{H}$  = Hessian matrix  
 $\hat{\mathbf{H}}$  = approximate Hessian matrix  
 $J$  = objective function  
 $\hat{J}$  = 2<sup>nd</sup> order approximation of  $J$   
 $k$  = time step counter  
 $\mathbf{P}$  = projection matrix  
 $p$  = pressure  
 $r$  = revenues/costs  
 $S$  = saturation  
 $t_k$  = time at timestep  $k$   
 $\mathbf{u}$  = input vector  
 $\mathbf{u}_0^*$  = optimal  $\mathbf{u}$  for  $J_1$   
 $\tilde{\mathbf{u}}_0^*$  =  $\mathbf{u}$  optimized for  $J_2$  constrained by  $\mathbf{B}$   
 $\tilde{\mathbf{u}}_0$  =  $\mathbf{u}$  optimized for  $J_2$  not constrained by  $\mathbf{B}$   
 $w$  = well constant  
 $\mathbf{x}$  = state vector  
 $\mathbf{x}_0$  = initial conditions  
 $\mathbf{y}$  = output vector  
 $\Delta t_k$  = time interval of time step  $k$   
 $\varepsilon$  = tolerance of optimality constraint  
 $\mu$  = viscosity  
 $\tau$  = step size of SA algorithm  
 $\tau_i$  = reference time  
 $\Phi$  = porosity  
 $\omega$  = weighting factor  
 $\Omega$  = weighting function  
 $\mathcal{S}$  = optimal subset of  $\mathcal{U}$   
 $\mathcal{U}$  = decision variable space

## Subscripts

$o$  = oil  
 $wf$  = flowing well bore  
 $wp$  = produced water  
 $wi$  = injected water  
 $cow$  = oil-water capillary  
 $1$  = primary  
 $2$  = secondary

## Superscripts

\* = optimal

## References

Asheim, H. 1988. Maximization of water sweep efficiency by controlling production and injection rates. Paper SPE 18365 presented at the SPE European Petroleum Conference, London, UK, October 16-18. DOI: 10.2118/18365-MS.

- Brouwer, D.R. and Jansen, J.D. 2004. Dynamic optimization of water flooding with smart wells using optimal control theory. *SPEJ* **9** (4): 391-402. DOI: 10.2118/78278-PA.
- Byrd, R.H. and Nocedal, J. 1990. An analysis of reduced Hessian methods for constrained optimization. *Mathematical Programming* **49** (1-3): 285-323. DOI: 10.1007/BF01588794.
- Chen, Y., Oliver, D.S. and Zhang, D. 2008. Efficient ensemble-based closed-loop production optimization. Paper SPE 112873 presented at the SPE/DOE Improved Oil Recovery Symposium, Tulsa, USA, 19-23 April, DOI: 10.2118/112873-MS.
- Haimes, Y.Y. and Li, D. 1988. Hierarchical multiobjective analysis for large-scale systems: Review and current status. *Automatica* **24** (1): 53-69. DOI: 10.1016/0005-1098(91)90120-Q.
- Huesman, A.E.M., Bosgra, O.H. and Van den Hof, P.M.J. 2007. Degrees of freedom analysis of economic dynamic optimal plantwide operation. In *Preprints 8th IFAC International Symposium on Dynamics and Control of Process Systems (DYCOPS) 1*: 165-170, Cancún, Mexico, 6-8 June.
- Jansen, J.D., Douma, S.G., Brouwer, D.R., Van den Hof, P.M.J., Bosgra, O.H. and Heemink, A.W. Closed-loop reservoir management. Paper SPE 119098 presented at the *2009 SPE Reservoir Simulation Symposium*, The Woodlands, Texas, U.S.A, 2-4 February. DOI: 10.2118/119098-MS.
- Kraaijevanger, J.F.B.M., Egberts, P.J.P., Valstar, J.R. and Buurman, H.W. 2007. Optimal water flood design using the adjoint method. Paper SPE 105764 presented at the *SPE Reservoir Simulation Symposium*, Houston, USA, 26-28 February. DOI: 10.2118/105764-MS.
- Marler, R.T. and Arora, J.S. 2004. Survey of multi-objective optimization methods for engineering. *Structural and Multidisciplinary Optimization* **26** (6): 369-395. DOI: 10.1007/s00158-003-0368-6.
- Naevdal, G., Brouwer, D.R. and Jansen, J.D. 2006. Water flooding using closed-loop control. *Computational Geosciences* **10** (1) 37-60. DOI: 10.1007/s10596-005-9010-6.
- Saputelli, L., Nikolaou, M. and Economides, M.J. 2005. Self-learning reservoir management. *SPEREE* **8** (6): 534-547. DOI: 10.2118/84064-PA.
- Saputelli, L., Nikolaou, M. and Economides, M.J. 2006. Real-time reservoir management: a multi-scale adaptive optimization and control approach. *Computational Geosciences* **10** (1) 61-96. DOI: 10.1007/s10596-005-9011-5.
- Sarma, P., Aziz, K. and Durlofsky, L.J. 2005. Implementation of adjoint solution for optimal control of smart wells. Paper SPE 92864 presented at the *SPE Reservoir Simulation Symposium*, Houston, USA, 31 January - 2 February. DOI: 10.2118/92864-MS.
- Sarma, P., Durlofsky, L.J. and Aziz, K.. 2008. Computational techniques for closed-loop reservoir modeling with application to a realistic reservoir. *Petroleum Science and Technology* **26** (10 & 11): 1120-1140. DOI: 10.1080/10916460701829580.
- Sudaryanto, B., and Yortsos, Y.C. 2000. Optimization of fluid front dynamics in porous media using rate control. *Physics of Fluids* **12** (7): 1656-1670.
- Srinivasan, B. Palanki, S. and Bonvin, D. 2003. Dynamic optimization of batch processes: I. characterization of the nominal solution. *Computers & Chemical Engineering* **27** (1): 1-26. DOI: 10.1016/S0098-1354(02)00116-3.
- Van Essen, G.M., Zandvliet, M.J., Van den Hof, P.M.J., Bosgra, O.H. and Jansen, J.D. 2006. Robust water flooding optimization of multiple geological scenarios. Paper SPE 102913 presented at the *SPE Annual Technical Conference and Exhibition*, San Antonio, USA, 24-27 September. DOI: 10.2118/102913-MS.
- Wang, C., Li, G. and Reynolds, A.C., 2009: Production optimization in closed-loop reservoir management. *SPEJ* **14** (3) 506-523. DOI: 10.2118/109805-PA.
- Zandvliet, M.J., Bosgra, O.H., Jansen, J.D., Van den Hof, P.M.J. and Kraaijevanger, J.F.B.M.. 2007. Bang-bang control and singular arcs in reservoir flooding. *Journal of Petroleum Science and Engineering* **58** (1 & 2): 186-200. DOI: 10.1016/j.petrol.2006.12.008.
- Zandvliet, M.J., van Doren, J.F.M., Bosgra, O.H., Jansen, J.D. and van den Hof, P.M.J. 2008. Controllability, observability and identifiability in single-phase porous media flow. *Computational Geosciences* **12** (4) 605-622. DOI: 10.1007/s10596-008-9100-3.